PAPER

Application of the recursive transfer method to flexural waves I: Novel discretization scheme using weak form theory framework and waveguide modes on inhomogeneous elastic plates

Hatsuhiro KATO[†a)], ***Member and*** **Hatsuyoshi KATO**[††], ***Nonmember***

SUMMARY Flexural waves on a thin elastic plate are governed by a fourth-order differential equation, which is not only attractive from a harmonic analysis point of view but also useful to realize an efficient numerical method for elastic materials. In this paper, two new idea s are proposed: one is an idea to use the tensor bases to describe flexural waves on inhomogeneous elastic plates and the other is a discretization method of the fourth-order differential equation based on the weak form theory framework. The proposing discretization method is of a preliminary consideration on the recursive transfer method (RTM) to analyze scattering problem of flexural waves. More than anything else, the proposing discretization method has a generality being applicable to any phenomena which can be formulated with the weak form theory. The accuracy of the difference equation derived by the discretization method is confirmed through comparing the analytical and numerical solutions of waveguide modes. As a typical problem to confirm the validity of the proposing difference equation, the influence of the spatially modulated elastic constant on waveguide modes is discussed.

key words: *Recursive transfer method, Elastic plate, Flexural wave, Weak form theory, Discretization*

1. Introduction

Recursive transfer method (RTM) is a numerical method that was developed to analyze electron waves in solids [1], [2] and was extended for microwave scattering problems [3], [4]. A notable feature of RTM is that it can extract localized waves around a scatterer [5], [6], whose theoretical scheme was constructed from a second-order difference equation being derived from a differential equation of motion by the Numerov's method [7]. Both of electron waves and microwaves are subject to a second-order differential equation, therefore, the Numerov's method serving for these waves is not applicable to flexural waves being governed by a fourth-order differential equation. Therefore, we have propose a new discretization method using the weak theory framework [8] which was developed to consider a boundary condition of waveguide wall [4].

In the present paper, the generality of the proposed discretization method is demonstrated through an analysis of the forth-order differential equation of the flexural waves on inhomogeneous plates. The inhomogenousness of a polymer film is controllable with the impurity implantation [9] and our discretization method will be useful to analyze and design flexural waves on the inhomogenous elastic plate. As an example to confirm the validity of our proposing discretization method, the influence of the spatially modulated elastic constant on waveguide modes is discussed. It is pointed out that the elastic constant modulation provides a feasible method to improve the efficiency of a micro-pump [10]–[13] that is composed of elastic plates. The compatibility of the discretization method with the recursive transfer method (RTM) is an important feature of our method, which will be also discussed in the another succeeding paper.

Theory being applicable to plates whose thickness varies uniaxially is already discussed [14], but the theory is not valid when the elastic constant varies spatially. Therefore, we propose new governing equation for the inhomogenous plate before developing the discretization method. It is notable that the tensor expression for the plate deformation [15], [25] is applied to derive the governing equation and formulate the weak form expression. The weak form formulation with our governing equation is compatible to the RTM procedure. Moreover, the expression of the energy flux [17] is extended to be valid for inhomogeneous plates.

For homogeneous elastic plates, the mode shapes on acoustic waveguides were discussed by several theories [18]–[21]. The influence of the uniaxial inhomogeneousness on mode shapes was also discussed to realize an attenuator that possesses a nonreflecting terminal [14] and the plate being composed of layered materials [22]. Our modal analysis is similar to the FE-BPM (Finite Element Beam Propagation Method) developed in fiber optics [23]. Since FE-BPM uses Crank-Nicolson method [24] for the discretization along the propagation axis, the resulting equation is difficult to solve by RTM because it is not the second-order difference equation. It is known that the numerical accuracy of the flexural wave analysis is not maintained if the degree of the interpolation polynomials is less than cubic [28]. On the other hand, our method can derive the second-order difference equation and it can achieve high accuracy because the weak form formulation can incorporate the high order interpolation technique.

The organization of this paper is as follows. In section 2, our new formulation about flexural waves on inhomogeneous plates is summarized. In section 3, the motion of flexural waves is formulated using the weak form theory

Manuscript received April **, 2012.

[†]The author is with the Interdisciplinary Graduate School of Medicine and Engineering, University of Yamanashi, Takeda, 4-3-11, Kofu, Yamanashi, 400-8511 Japan.

[††]The author is with the Tomakomai National College of Technology, 433, Nishikioka, Tomakomai, Hokkaido, 059-1275, Japan.

a) E-mail: katoh@yamanashi.ac.jp

DOI: 10.1587/transfun.E97.A.1075

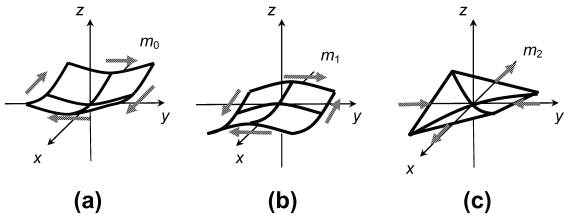

Fig. 1 Plate deformations involved by moment components m_0, m_1 and m_2.

framework and a governing difference equation for flexural waves is derived through discritizing this functional. In section 4, to confirm the accuracy of the proposing method, the numerically obtained dispersion relation and mode shapes in a uniform waveguide are compared to the analytic solution. The influence of the plate inhomogeneousness on mode shapes is also discussed considering a uniaxial variation of the elastic constant. Last section is devoted to the conclusion. In Appendix A, an identity relation for weak form formulation is derived. In Appendix B, the analytic detail of the discretization procedure is summarized. Considering the rotary inertia of the plate, the analytic mode shapes and dispersion relation is summarized in Appendix C.

2. Flexural wave on inhomogeneous plates

2.1 Tensor expressions for the flexural motion

2.1.1 Three elements of the flexural deformation

Let us consider a thin elastic plate located on the xy-plane, whose displacement along the z-axis is denoted by $u(x, y)$. The first-order and second-order derivatives of $u(x, y)$ are related to the rotation and flexural deformation of plates, respectively. The second-order derivatives of $u(x, y)$ compose the Hessian $Hu(x, y)$ that is defined as follows,

$$Hu = \begin{bmatrix} \frac{\partial^2}{\partial x^2}u & \frac{\partial^2}{\partial x \partial y}u \\ \frac{\partial^2}{\partial y \partial x}u & \frac{\partial^2}{\partial y^2}u \end{bmatrix}. \tag{1}$$

The Hessian is a tensor and belongs to the linear space of 2×2 matrices. Any second-order tensor can be generated by linearly independent matrices, or the tensor bases, defined as follows,

$$\hat{1} = \begin{bmatrix} 1 & 0 \\ 0 & 1 \end{bmatrix}, \hat{\sigma} = \begin{bmatrix} 0 & 1 \\ -1 & 0 \end{bmatrix}, \tag{2}$$

$$\hat{\tau} = \begin{bmatrix} 0 & 1 \\ 1 & 0 \end{bmatrix}, \hat{v} = \begin{bmatrix} 1 & 0 \\ 0 & -1 \end{bmatrix}. \tag{3}$$

The inner product $\langle X, Y\rangle$ between two elements X and Y in the linear space is introduced as $\langle X, Y\rangle = \mathrm{tr}[X^T Y]$, then the bases $\hat{1}, \hat{\sigma}, \hat{\tau}$ and $\hat{v}$ become orthogonal under this inner product [15], [16].

The Hessian is a symmetric tensor which can be expressed by a linear combination of the tensor bases as follows,

$$Hu = \frac{\Delta_0 u}{2}\hat{1} + \frac{\Delta_1 u}{2}\hat{v} + \frac{\Delta_2 u}{2}\hat{\tau}. \tag{4}$$

Here, the elements $\Delta_p u(x, y)$ $(p = 0, 1, 2)$ are defined with the nabla $\nabla = [\partial/\partial x\ \partial/\partial y]^T$ as follows,

$$\Delta_0 u = \nabla \cdot \nabla u = \frac{\partial^2 u}{\partial x^2} + \frac{\partial^2 u}{\partial y^2}, \tag{5}$$

$$\Delta_1 u = \nabla \cdot \hat{v}\nabla u = \frac{\partial^2 u}{\partial x^2} - \frac{\partial^2 u}{\partial y^2}, \tag{6}$$

$$\Delta_2 u = \nabla \cdot \hat{\tau}\nabla u = 2\frac{\partial^2 u}{\partial x \partial y}. \tag{7}$$

The operator Δ_0 is identical to a well known operator of the Laplacian. These three elements can be regarded as a kind of strains induced by the flexural deformation, and it is easy to show that these three satisfy the following relation,

$$\nabla\Delta_0 u = \hat{v}\nabla\Delta_1 u + \hat{\tau}\nabla\Delta_2 u, \tag{8}$$

which is the compatibility condition of the flexural deformations.

2.1.2 Moment elements

When a plate is assumed to be isotropic, the elements of a moment tensor $M(x, y) = [m_{pq}(x, y)]$ $(p, q = x, y)$ can be expressed with the second-order derivatives of $u(x, y)$ as follows [21],

$$m_{xx} = D\left(\frac{\partial^2 u}{\partial x^2} + \nu\frac{\partial^2 u}{\partial y^2}\right), \tag{9}$$

$$m_{yy} = D\left(\frac{\partial^2 u}{\partial y^2} + \nu\frac{\partial^2 u}{\partial x^2}\right), \tag{10}$$

$$m_{xy} = m_{yx} = (1 - \nu)D\frac{\partial^2 u}{\partial x \partial y}, \tag{11}$$

where the $D(x, y)$ is the stiffness constant of flexural deformations and is defined as $D = Eb^3/[12(1 - \nu^2)]$ with the Young's modulus $E(x, y)$, the Poisson's ratio $\nu(x, y)$, and the plate thickness $b(x, y)$. These relations were obtained for homogenous plates, but the same formulae are valid for inhomogeneous plates where the material constants and the plate thickness are allowed to be dependent on the coordinates. Further, the moment tensor M is also expressed in an another form as follows,

$$M = m_0\hat{1} + m_1\hat{v} + m_2\hat{\tau}, \tag{12}$$

where the elements m_r $(r = 0, 1, 2)$ are defined by $m_0 = (m_{xx} + m_{yy})/2$, $m_1 = (m_{xx} - m_{yy})/2$, $m_2 = m_{xy} = m_{yx}$. Using these relations, new expressions of the tensor elements, m_r, are found as follows,

$$m_r = D_r\Delta_r u, \tag{13}$$

where $D_r(x, y)$ are variants of the stiffness constant defined as follows,

$$D_0 = \frac{1}{2}(1+\nu)D, \quad D_1 = D_2 = \frac{1}{2}(1-\nu)D. \tag{14}$$

In Fig. 1, the flexural deformation and moment component $m_r(x, y)$ caused by $\Delta_r u$ ($r = 0,1,2$) are shown when the plate is isotropic. The moment components m_r are denoted by the arrows around the fringe of the rectangular plate element. The direction of the arrows is aligned with the thumb of the right hand when the the other four fingers are wound along the bending direction.

The expressions with m_r are not only highly symmetric but also useful to derive a governing equation of inhomogeneous elastic plates. Although the moment expression with the Hessian components is already known [25], this is the first proposal to apply the moment expression (12) to the dynamic formulation of the flexural wave.

2.2 Governing equation for inhomogeneous plates

2.2.1 Moment balance and shear force

Let us consider an infinitesimal plate element extracted imaginarily from a plate as shown in Fig. 2, where A is the projection of the element on xy-plane at the two-dimensional position vector $\mathbf{r}_A$, $\mathbf{n}$ and $d\ell$ are the normal vector and infinitesimal length on the boundary ∂A, respectively. The shear force $s(x, y)$ and the moment vector $\mathbf{m}(x.y)$ per unit length along the element boundary are given by $s = \mathbf{s}\cdot\mathbf{n}$ and $\mathbf{m} = \hat{\sigma}M\mathbf{n}$ with the shear force vector $\mathbf{s} = [s_x, s_y]^T$ and the moment tensor $M(x, y)$, respectively. Here, the elements s_x and s_y are the shear force acting on the plate cross section whose normal vector is parallel to the x- and y-axis, respectively. The positive direction of shear force is defined to be anti-parallel to the z-axis. The pair of the elements $[s_x\ s_y]^T$ follows the transformation rule of the vector under the coordinate transformation, though it is not always obvious [20].

The shear forces $s = \mathbf{s}\cdot\mathbf{n}$ acting at the position $\mathbf{r}$ on the boundary ∂A involves the moment vector around the position $\mathbf{r}_A$, which is expressed as $-\hat{\sigma}(\mathbf{r}-\mathbf{r}_A)\mathbf{s}\cdot\mathbf{n}$. Using the fact that the area of the element A is infinitesimal and considering up to linear terms, the total moment $\mathbf{m}_A$ from the whole boundary ∂A is expressed as

$$\begin{aligned}\mathbf{m}_A &= \int_{\partial A}\left\{-\hat{\sigma}(\mathbf{r}-\mathbf{r}_A)\mathbf{s}\cdot\mathbf{n} + \hat{\sigma}M\mathbf{n}\right\}d\ell \\ &\approx \hat{\sigma}(-\mathbf{s} + \nabla * M)dS.\end{aligned} \tag{15}$$

At the transformation from the first line to the second in the right hand side, the Gauss' theorem about the tensor fields [29] is applied and the symbol $\nabla * M$ stands for the vector field which is reduced from the tensor M such as $\nabla * M = \nabla m_0 + \hat{\upsilon}\nabla m_1 + \hat{\tau}\nabla m_2$. The vector field $\nabla * M$ is called the divergence of the tensor filed that is identical to the quantity defined such as $[\sum_q \frac{\partial}{\partial x_q} T_{pq}]$ with the rectangular coordinates [29].

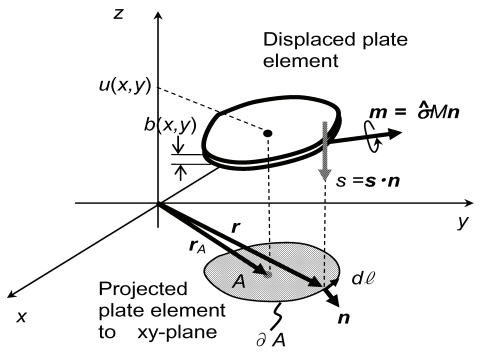

Fig. 2 Infinitesimal plate element with the geometrical and elastic quantities.

If the infinitesimal element A is regarded as a rigid body, the angular velocity vector of A is approximately equal to $\hat{\sigma}\nabla\dot{u}$, where the super dot, $\dot{}$, stands for the time derivative. Then, the angular momentum $\mathbf{L}_A$ can be expressed as follows,

$$\mathbf{L}_A = \hat{\sigma}\rho I\nabla\dot{u}dS. \tag{16}$$

Here, $I(x, y) = b(x, y)^3/12$ is the second area moment of the cross section, which is valid when the neutral stress axis is located at the plate centre.

Using the moment balance $\mathbf{m}_A = \dot{\mathbf{L}}_A$ and substituting (15) and (16) for $\mathbf{m}_A$ and $\mathbf{L}_A$, respectively, the expression of the shear vector $\mathbf{s}$ can be derived as follows,

$$\mathbf{s} = \nabla m_0 + \hat{\upsilon}\nabla m_1 + \hat{\tau}\nabla m_2 - \rho I\nabla\ddot{u}. \tag{17}$$

2.2.2 Force balance and governing equation

The governing equation of the flexural motion can be derived through taking a balance between the inertia force $-\rho b\ddot{u}$ and the shear forces $\mathbf{s}\cdot\mathbf{n}$ that acts on the boundary of the infinitesimal element A. The balance between the forces is expressed in the integral form as follows,

$$\int_{\partial A}\mathbf{s}\cdot\mathbf{n}d\ell = -\int_A \rho b\ddot{u}dS. \tag{18}$$

Applying the Gauss' theorem on the integral in the left hand side of (18) and using the fact that the shape of the element A is arbitrary, one can find the relation $\nabla\cdot\mathbf{s}+\rho b\ddot{u} = 0$, which is equivalent to

$$\Delta_0 m_0 + \Delta_1 m_1 + \Delta_2 m_2 - \rho I\Delta_0\ddot{u} + \rho b\ddot{u} = 0. \tag{19}$$

This is the governing equation of flexural waves on inhomogeneous elastic plates. When a wave is in steady state with an angular frequency of ω, the equation reduces to

$$\Delta_0 m_0 + \Delta_1 m_1 + \Delta_2 m_2 + \rho\omega^2 I\Delta_0 u - \rho\omega^2 bu = 0. \tag{20}$$

If the plate is homogeneous, the terms including $\Delta_1 u$ and $\Delta_2 u$ in the governing equation (19) or (20) are unified into the term with $\Delta_0 u$ through the compatibility condition (8)

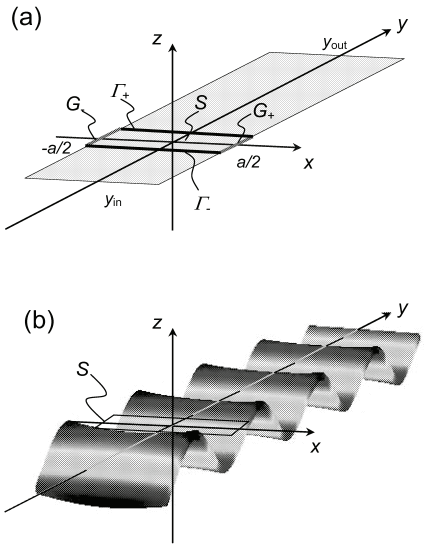

Fig. 3 Waveguide configuration. (a) The coordinate and integration region S. (b) Wave shape in the symmetric mode S_0.

as shown by (A·34) in Appendix C. Furthermore, if the rotary inertia is also negligible ($I = 0$), the governing equation results in the equation of the Kirchhoff theory [20].

3. Discretization following weak form theory framework

3.1 Functional for flexural waves and the energy flux

As shown in Fig. 3, a flexural wave is assumed to be traveling along a waveguide of the width a. The x- and y-axes are set along the width and length directions of the waveguide, respectively. In this section, a functional is defined in the narrow region $S = \{(x, y), |x| < a/2, |y| < h_y\}$ around the origin $y = 0$, but the same discussion is valid at any site being shifted along the y-axis. According to the weak form theory framework [28], we derive the following functional,

$$F = \int_S \Big(m_0\Delta_0 w + m_1\Delta_1 w + m_2\Delta_2 w - \rho\omega^2 I\nabla u\cdot\nabla w - \rho\omega^2 buw\Big)dxdy + \sum_{\varsigma=\pm}\int_{\Gamma_\varsigma}\Big(V_y w - M_y\frac{\partial w}{\partial y}\Big)dx. \quad (21)$$

This is obtained according to the following two steps: (i) Multiplying an arbitrary test function $w(x, y)$ to both sides of the equation (20) and integrating at the region S. (ii) Applying the following identity relation,

$$(\nabla\cdot\mathbf{s})w = m_0\Delta_0 w + m_1\Delta_1 w + m_2\Delta_2 w - \rho I\omega^2\nabla u\cdot\nabla w + \nabla\cdot\big(\mathbf{s}w - M\nabla w\big), \quad (22)$$

to obtain the linear integrals about the boundaries $\Gamma_\pm$ in (21). The derivation of the identity is geven in Appendix A. The lines $\Gamma_\pm = \{(x, y), |x| < a/2, y = \pm h_y\}$ are parts of whole boundary ∂S, which are perpendicular to the y-axis. The moment M_y and the Kirchhoff's effective shear force V_y on the boundary are expressed as $M_y = m_0 - m_1$ and $V_y = s_y + \frac{\partial}{\partial x}m_2$, respectively [20]. The shear forces and the moments at the boundaries $G_\pm = \{(x, y), x = \pm a/2, |y| \le h_y\}$ are eliminated with the assumption that the fringe of the wave guide is not restricted.

If the following condition is imposed on the arbitrary function $w(x, y)$ such as,

$$w(x, \pm h_y) = 0,\ \frac{\partial}{\partial y}w(x, \pm h_y) = 0, \quad (23)$$

the terms in (21) relating to the boundaries $\Gamma_\pm$ vanish. Then, no natural condition is imposed on the function $u(x, y)$ at the boundaries under the null value problem. Here, the null value problem is stated as follows: 'what is the function $u(x, y)$ which satisfies the condition $F[w, u] = 0$ for any arbitrary function $w(x, y)$?', which is equivalent to find the solution of (20).

Using the identity relation (22) with substitution of the displacement $u(x, y)$ for the arbitrary function $w(x, y)$, the energy flux $\mathbf{J}$ defined by Bobrovnitskii [17] for the case of homogenous plates is extended to the inhomogeneous case as follows,

$$\mathbf{J} = \mathbf{s}\dot{u} - M\nabla\dot{u}. \quad (24)$$

A point-wise expression of the energy conservation is given as $\dot{\epsilon} + \nabla\cdot\mathbf{J} = 0$ with the total energy ϵ composed of the kinetic energy $\rho\dot{u}^2/2$ and the elastic potential $\langle Hu, Mu\rangle/2$. Here, note that the moment tensor defined by Bobrocskii is $\hat{\sigma}M$ in our denotations.

3.2 Interpolation of the field variables

The functional (21) can be discretized through interpolating the spatially discretized field values at lattice points. Let us divide the xy-plane into the rectangular lattice with the step sizes h_x and h_y, then the lattice points are assigned by indexes $\ell(= 0, 1, 2, ..., N_x)$ and $n(= -1, 0, 1)$ as follows,

$$x_\ell = -a/2 + \ell h_x, \quad (25)$$

$$y_n = nh_y. \quad (26)$$

Here, the waveguide of the width a is assumed to be divided into N_x parts and the step size $h_x = a/N_x$. The step size h_y and the index n are already introduced in the previous section relating to the region S. Then, the functional (21) can be expressed with the spatially discretized field values at the lattice points, $u(x_\ell, y_n)$ and $w(x_\ell, y_n)$.

It is known that the plate deformation should be interpolated at least with cubic polynomials to analyze the flexural wave [28]. Therefore, we use the Hermite interpolation functions $L_0(\eta), N_0(\eta), L_1(\eta)$ and $N_1(\eta)$, which are cubic polynomials defined at the interval $0 \le \eta \le 1$ and satisfy the following conditions,

$$L_0(0) = L_1(1) = h_y^{-1}N_0'(0) = h_y^{-1}N_1'(1) = 1, \quad (27)$$

$$L_0(1) = L_1(0) = N_0'(1) = N_1'(0) = 0, \quad (28)$$

$$L_0'(0) = L_1'(1) = N_0(0) = N_1(1) = 0, \quad (29)$$

$$L_0'(1) = L_1'(0) = N_0(1) = N_1(0) = 0. \quad (30)$$

Here, the dash, $'$, stands for the derivative with respect to η. The values of these functions are set to be null at the regions $\eta < 0$ and $\eta > 1$. Using these interpolation functions and the two-dimensional vector defined by $\mathbf{u}_n(x) = [u(x, y_n)\ \frac{\partial}{\partial y}u(x, y_n)]^T$ the field variable $u(x, y)$ is interpolated as follows,

$$u(x,y) = \sum_{n=-1}^{0} \Big\{ \Big[L_0(\eta_n)\ N_0(\eta_n) \Big] \mathbf{u}_n(x) + \Big[L_1(\eta_n)\ N_1(\eta_n) \Big] \mathbf{u}_{n+1}(x) \Big\}, \quad (31)$$

with $\eta_n = (y - nh_y)/h_y$. Moreover, using the four dimensional vector

$$\mathbf{U}_n(x_\ell) = [\mathbf{u}_n(x_\ell)\ \frac{\partial}{\partial x}\mathbf{u}_n(x_\ell)]^T \quad (32)$$

and the variable $\xi_\ell = (x - \ell h_x)/h_x$, the interpolation about the variable x is also realized as follows,

$$\mathbf{u}_n(x) = \sum_{n=-1}^{0} \Big\{ \Big[L_0(\xi_\ell)\ N_0(\xi_\ell) \Big] \mathbf{U}_n(x_\ell) + \Big[L_1(\xi_\ell)\ N_1(\xi_\ell) \Big] \mathbf{U}_n(x_{\ell+1}) \Big\}. \quad (33)$$

As the same manner, using the vectors $\mathbf{w}_0(x) = [w(x, 0)\ \frac{\partial}{\partial y}w(x, 0)]^T$ and $\mathbf{W}_0(x_\ell) = [\mathbf{w}_0(x_\ell)\ \frac{\partial}{\partial x}\mathbf{w}_0(x_\ell)]^T$, the arbitrary function $w(x.y)$ is also interpolated as follows,

$$w(x,y) = \Big[L_1(\eta_{-1})\ N_1(\eta_{-1}) \Big] \mathbf{w}_0(x) + \Big[L_0(\eta_0)\ N_0(\eta_0) \Big] \mathbf{w}_0(x) \quad (34)$$

$$\mathbf{w}_0(x) = \sum_{\ell=0}^{N_x-1} \Big\{ \Big[L_0(\xi_\ell)\ N_0(\xi_\ell) \Big] \mathbf{W}_0(x_\ell) + \Big[L_1(\xi_\ell)\ N_1(\xi_\ell) \Big] \mathbf{W}_0(x_{\ell+1}) \Big\}. \quad (35)$$

Here, the condition that the function $\mathbf{w}_n(x)$ vanishes at $n = \pm 1$, *i.e.* $\mathbf{w}_{\pm 1}(x) = 0$, is used, which is required to satisfy the boundary condition (23).

Let us introduce the function symbol $f(x, y)$ to represent any of $b(x, y)$, $I(x, y)$, and $D_r(x, y)$ (r=0, 1, 2), and interpolate the function $f(x, y)$ as as follows,

$$f(x,y) = \sum_{n=-1}^{0}\sum_{\ell=0}^{N_x-1} \theta(\xi_\ell)\theta(\eta_n) f(x_n + \frac{h_x}{2}, y_\ell + \frac{h_y}{2}). \quad (36)$$

Here, the function $\theta(\xi)$ is a discontinuoius step-wise function that is defined for the variable ξ such as,

$$\theta(\xi) = \begin{cases} 0 & (\xi < 0, \xi > 1) \\ 1 & (0 \le \xi \le 1) \end{cases} . \quad (37)$$

Though the interpolation expression (36) may be discontinous at the contour of the lattice square, the deterioration of the discretization accuracy is minute because the functional (21) does not include any derivative of the functions.

3.3 Derivation of the difference equation

When the functions in the expression (21) are replaced by the interpolated expressions (31), ..., (36), all integrals in (21) can be performed analytically because all functions are interpolated by the polynomials of x and y. Ultimately, the integrated expression contains the spatially discretized field values, which can be regarded as a discretization of the functional. Let us consider a vector $\mathbf{\Phi}_n$ to be composed of spatially discretized values of the field variables $\mathbf{U}_n(x_\ell)$ defined by (32) and its derivative $\frac{\partial}{\partial x}\mathbf{U}_n(x_\ell)$ (ℓ = 0, 1 ,... ,N_x). Then, the vector $\mathbf{\Phi}_n$ is a column vector of $4(N_x+1)$ dimension, which is denoted concisely such as $\mathbf{\Phi}_n = \{[\mathbf{U}_n(x_\ell)\ \frac{\partial}{\partial x}\mathbf{U}_n(x_\ell)]^T\}$. Here, the brackets, { }, mean a column vector whose elements are generated by varying the index ℓ over its whole range. A similar column vector about the arbitrary function $w(x, y)$ can be defined such as $\mathbf{\Psi}_0 = \{[\mathbf{W}_0(x_\ell)\ \frac{\partial}{\partial x}\mathbf{W}_0(x_\ell)]^T\}$. Using the vectors $\mathbf{\Phi}_n$ and $\mathbf{\Psi}_0$ and introducing matrices $\bar{c}_0, \bar{b}_0$, and $\bar{a}_0$, the functional $F[w, u]$ can be expressed as $F[w.u] = \mathbf{\Psi}_0^T[\bar{c}_0\ \bar{b}_0\ \bar{a}_0][\mathbf{\Phi}_{-1}\ \mathbf{\Phi}_0\ \mathbf{\Phi}_1]^T$. The symbol with the super bar, $\bar{}$, is for the $4(N_x+1)\times 4(N_x+1)$ matrix. The detail to derive this expression is summarized in Appendix B. Because the functional F is bilinear about $\mathbf{\Psi}_0$ and $\mathbf{\Phi}_n$, the condition that the functional takes the value $F[w, u] = 0$ for arbitrary function $w(x, y)$ is expressed as $\bar{c}_0\mathbf{\Phi}_{-1} + \bar{b}_0\mathbf{\Phi}_0 + \bar{a}_0\mathbf{\Phi}_1 = 0$.

Until now the centre of the region S is assumed to be at the origin $y = 0$, but the same discussion is possible for any centre at $y_n = nh_y$ ($n = 0, \pm 1, \pm 2, ...$). Therefore, the translation of the centre to the site y_n leads to the following general expression,

$$\bar{c}_n\mathbf{\Phi}_{n-1} + \bar{b}_n\mathbf{\Phi}_n + \bar{a}_n\mathbf{\Phi}_{n+1} = 0, \quad (38)$$

where the matrices $\bar{c}_0, \bar{b}_0$, and $\bar{a}_0$ are replaced with $\bar{c}_n$, $\bar{b}_n$, and $\bar{a}_n$, and the vectors $\mathbf{\Phi}_0$ and $\mathbf{\Phi}_{\pm 1}$ are substituted for $\mathbf{\Phi}_n$ and $\mathbf{\Phi}_{n\pm 1}$, respectively. This is the second-order difference equation governing the flexural waves on inhomogeneous plates.

Because the original differential equation (20) contains the term ω^2, the functional (21) can be divided into two parts which include and do not include the terms proportional to ω^2. Therefore, the coefficient matrices also can be divided into two parts and expressed such as $\bar{c}_n = \bar{c}_n^{(1)} - \omega^2\bar{c}_n^{(2)}$, $\bar{b}_n = \bar{b}_n^{(1)} - \omega^2\bar{b}_n^{(2)}$ and $\bar{a}_n = \bar{a}_n^{(1)} - \omega^2\bar{a}_n^{(2)}$, as derived in Appendix B. The difference equation (38) is also divided with respect to ω^2 as follows,

$$\bar{c}_n^{(1)}\mathbf{\Phi}_{n-1} + \bar{b}_n^{(1)}\mathbf{\Phi}_n + \bar{a}_n^{(1)}\mathbf{\Phi}_{n+1} = \omega^2\Big(\bar{c}_n^{(2)}\mathbf{\Phi}_{n-1} + \bar{b}_n^{(2)}\mathbf{\Phi}_n + \bar{a}_n^{(2)}\mathbf{\Phi}_{n+1}\Big). \quad (39)$$

This expression will be used to obtain waveguide modes in the next section.

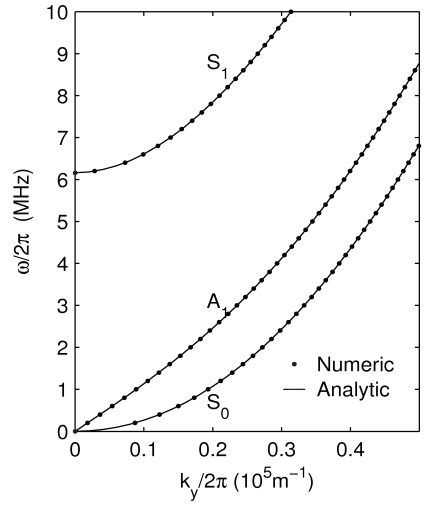

Fig. 4 Dispersion relation of waveguide modes

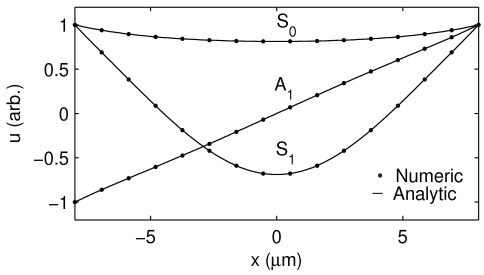

Fig. 5 Comparison of mode shape functions being obtained by numerical and analytical methods.

4. Waveguide mode

4.1 Mode function as an eigenvector

If the flexural wave with a wave number k_y travels steadily in a waveguide along the y-axis, the displacement $u(x, y)$ due to the flexural deformation is expressed as $u(x, y) = X(x)e^{ik_y y}$ with the mode shape function $X(x)$. At the steady state, the n dependence of the vector $\mathbf{\Phi}_n$ in the equation (39) is also given in a similar form such as $\mathbf{\Phi}_n = e^{i\tilde{k}_y h_y n}\hat{\mathbf{\Phi}}_X$, where $\hat{\mathbf{\Phi}}_X$ is a $4(N_y + 1)$-dimensional vector and does not depend on n. Substituting this form for $\mathbf{\Phi}_n$ in the difference equation (39) leads to the following equation,

$$A\hat{\mathbf{\Phi}}_X = \omega^2 B\hat{\mathbf{\Phi}}_X, \tag{40}$$

$$A = \bar{c}_0^{(1)}e^{-ik_y h_y} + \bar{b}_0^{(1)} + \bar{a}_0^{(1)}e^{ik_y h_y}, \tag{41}$$

$$B = \bar{c}_0^{(2)}e^{-ik_y h_y} + \bar{b}_0^{(2)} + \bar{a}_0^{(2)}e^{ik_y h_y}, \tag{42}$$

where the index n is assumed to be $n = 0$ because of the translational invariance. This is one of the generalized eigenvalue problem where ω^2 is the eigenvalue and $\hat{\mathbf{\Phi}}_X$ is the eigenvector. The spatially discretized value of the mode function, $X(x_\ell)$ ($\ell = 0, 1, 2, ..., N_x$), is the $(4\ell + 1)$-th component of the vector $\hat{\mathbf{\Phi}}_X$.

In Fig. 4, to estimate the accuracy of the numerical solution, the dispersion relations in a homogeneous plate are shown, where the numerical and analytical data are depicted with dots and solid lines, respectively. The horizontal and vertical axis is equivalent to the frequency $f(= \omega/2\pi)$ and inverse of the wave length along the y-axis$1/\lambda_y(= k_y/2\pi)$, respectively. Details to derive the analytic dispersion relation are summarized in Appendix C. The elastic plate is assumed to be composed of PMMA (polymethyl-methacrylate), whose organic property attracts an attention as a film material [9]. The material constants are chosen as follows: Young's modulus $E = 25$ GPa, Poisson's ratio $\nu = 0.35$ and mass density $\rho = 1.19$ g/cm^3. The geometrical dimensions of the wave guide and the disretization parameters are as follows: The waveguide width $a = 16$ μm, plate thickness $b = 1$ μm, discrete step sizes $h_x = 0.64$ μm and $h_y = 0.66$ μm. The dispersion curves labeled with S_0 and S_1 are for modes which is symmetric with respect to the x-axis inversion and the curve with A_1 is for the antisymmetric mode. The discrepancy between the numerical and analytical values is less than 0.00247 MHz that is about 1/2500 as compared with the S_1 mode frequency at $k_y = 0$, *i. e.*, $f_{\mathrm{min}S_1} = 6.23$ MHz.

Possible quantities to be used for converting the governing equation to non-dimensional form are the wave number k_{EB} and the frequency f_{EB} of the Euler-Bernoulli beam [20]; Those are given by $k_{\mathrm{EB}} = (\rho b\omega^2/D)^{1/4}$ and $f_{\mathrm{EB}} = (2\alpha^2/\pi a^2)\sqrt{D/\rho b}$ where $\alpha(=2.365)$ is a solution of $\tan\alpha + \tanh\alpha = 0$. The values are $k_{\mathrm{BE}} = 2.37 \times 10^5$ m^{-1} at $f = 4$ MHz and $f_{\mathrm{EB}} = 6.21$ MHz. Here, it is noticed that the discripancy between $f_{\mathrm{min}S_1}$ and f_{EB} is caused by the rotarlly inertia included in the geverning equation (20).

In Fig. 5, the mode shapes are also shown when the wave number is $k_y = 2.4 \times 10^5$ m^{-1} that corresponds to the frequencies of 4.00 MHz, 5.84 MHz, and 11.7 MHz for S_0, A_1, and S_1 modes, respectively. The numerically and the analytically obtained data are also shown by dots and solid lines, respectively. The maximum amplitude of each mode shape is normalized so as to be unity. The discrepancy between the numerical and analytical values is less than 1/3400 in the normalized scale.

The numerical data of both dispersion curves and mode shapes acculatelly trace the analytical data within the relative error 1/2500, which gives an convince for a practical use of our proposing method.

4.2 Inhomogeneousness influence on mode shapes

The shape of the symmetric mode S_0 is turned up at waveguide fringes because of lateral deformations caused by the Poisson's ratio. As an example to demonstrate the validity of our new equation (20), the suppression of the fringe turning with the inhomogenous stiffness distribution is discussed in this section.

In Fig.4, the suppression of the fringe turning is shown

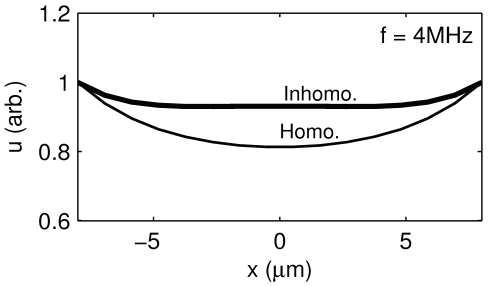

Fig. 6 Influence of inflnhomogeneousness on S_0 mode shape.

when the stiffness D varies uniaxially. The stiffness modulation is assumed to be caused by the spatially modulated Young's modulus $E(x)$ which is defined as follows,

$$E(x) = E_0\{1 + (2x/a)^8\}. \tag{43}$$

Here, the value of the parameter E_0 (= 25 GPa) is identical to the Young's modulus used to obtain the curves in Fig. 5. The thick line is for the inhomogeneous case with the modulus defined by (43) and the thin line is for the homogeneous case which is equivalent to the curve in Fig. 5. The frequency is assumed to be 4 MHz.

It is known that the efficiency of a micro-pump being composed of plates deteriorates because of the fringe turning of the mode shape and the flattened mode shape may improve the efficiency [12], [13]. The modulation by the spatially varying elastic constant provides a feasible method to control the mode shapes because the modulation of the Young's modulus is already realized by an impurity implantation [9]. More than anything else, the impurities do not influence the plate flatness compared with cutting works.

5. Conclusion

In order to extend the scope of RTM, we developed a discretization method to convert the fourth-order differential equation into the second-order difference equation using the weak form theory framework. The theory proposed in this paper is valid for flexural waves generated on inhomogeneous and isotropic elastic plates where not only plate thicknesses but also elastic constants depend on the coordinates. The accuracy of the numerical solution of the difference equation is confirmed through the comparison with the analytical solutions for an acoustic waveguide composed of a homogeneous plate. The discrepancy between the numerically and analytically obtained values of the mode function is less than 1/2500 in the normalized scale. As a feasible method to control the mode shape, an effect of the stiffness modulation through the Young's modulus is pointed out.

To demonstrate the validity of RTM for flexural waves, we are preparing another paper to solve a scattering problem using our difference equation in relating to the localized wave. The waveguide modes discussed in the present paper has full compatibility to RTM.

Acknowledgment

This research is supported by JSPS KAKENHI(23560065).

References

[1] J. A. Appelbaum and D. R. Hamann, "Self-consistent electronic structure of solid surfaces", Physical Review B, vol. 6, no. 6, pp. 2166-2177, Sept. 1972.
[2] K. Hirose and M. Tsukada, "First-principles calculation of the electronic structure for a bielectrode junction system under strong field and current", Physical Review B, vol.51, no.8, pp.5278-5290, Feb. 1995.
[3] H. Kato, M. Kitani and H. Kato, "Recursive transfer method as an accurate numerical method to analyze the scattering of the electromagnetic wave", IEICE Trans. Electron. (Japanese Edition), vol.J94-C, pp.1-9, 2011.
[4] H. Kato and H. Kato, "A new formalization for the recursive transfer method using the weak form theory framework and its application to microwave scattering ", submiting to IEICE Trans. Fundamentals.
[5] H. Kato and Y. Kanno, "An analysis on Microwave Absorption of the Catalyst in a Thermal Decomposition Reaction by the Recursive Transfer Method", Japanese Journal of Applied Physics, vol.47, no. 6, pp. 4846-4850, 2008.
[6] H. Kato, M. Kitani and H. Kato, "Proposal of recursive transfer method as an accurate numerical method for microwave scattering Problem", Proc. Asia-Pacific Radio Science Conference, Japan, no. BEFKc-2, Sept. 2010.
[7] F. Y. Hąji, H. Kobeisse and N. R. Nassif, "On the numerical solution of shroedinger's radial equation", Journal of Computational Physics, vol. 16, pp. 150-159, 1974.
[8] J. Fish and T. Belytshko, A first course of finite elements, chap. 6, Joh Wiley & Sons, Chichester, 2007.
[9] K. Yamazaki, T. Yamaguchi and H. Yamaguchi, "Modulation of Young's modulus of poly(methyl methacrylate) nano beam", Japanese Journal of Applied Physics, vol. 46, no. 49, pp. L1225-L1227, 2007.
[10] T. Honda, J. Yamasaki and K. I. Arai, "Fabrication and testing of a small pump composed of a magnet and an elastic plate", IEEE Transactions on Magnetics, vol. 34, Issure 4, 1998.
[11] Y. Wada, D. Koyama and K. Nakamura, "Finite element analysis of acoustic streaming in an ultrasonic air pump", Japanese Journal of Applied Physics, vol. 49, article 07HE15, 2010.
[12] K. Yoneyama, Y. Shibata and Y. Matsumura, "Air blower using traveling space generated between two resonantly-driven plates", Proc. 2010 JSME Conf. on Robotics and Mechtronics (Japanese Edition), no. 1P1-A21, Japan, June 2010.
[13] I. Iwamoto, Y. Matsumura, and K. Yoneyama, "Transportation using travelling space generated between two resonanttly-driven plates", Proc. of JISME Dynamic and Design Conf. (Japanese Edition), article 567, Sapporo, 2009.
[14] V. V. Krylov and F. J. B. Tilman, "Acoustic 'black holes' for flexural waves as effective vibration dampers", Journal of sound and vibration, vol. 274, pp. 605-619, 2004.
[15] Y. Yamauchi and M. Sugiura, Introduction to continuum groups, p.14, Baifukan (Japnanese ed.), Tokyo, 1960.
[16] H. F. Jones, Groups, Representations and Physics (2nd ed.), Taylor & Fransic, New York, 1998.
[17] Yu. I. Bobrovnitskii, "Calculation of the power flow in flexural waves on thin plates", Journal of Sound and Vibration, vol. 149, no. 1, pp. 103-106, 1996.
[18] B. A. Auld, Acoustic fields and waves in solids (volume II), Wiley Interscience, New York, 1973.
[19] C. Vermula and A. N. Noris, "Flexural wave propagation and scattering on thin plates using Mindlin theory", Wave Motion, vol. 26, pp.1-12, 1997.
[20] K. F. Graff, Wave motion in elastic solids, chp. 4, Oxford Unv. Press, London 1975.
[21] S. Timoshenko, and S. Woinowsky-Krieger, Theory of plate and shell (2nd ed.), chap. 4, McGraw-Hill, New York, 1959.
[22] C. Vemura, A. N. Noris, and G. D. Cody, "Attenuation of waves in plates and bars using a graded impedance interface at edges", Journal of Sound and Vibration, vol. 196, no. 1, pp. 107-117, 1996.
[23] M. Koshiba, "Beam propagation method based on finit element scheme and its application to optical waveguide analysis", IEICE Trans. Electron. (Japanese Edition), vol. J82-C-II, no. 11, pp. 599-608,1999.
[24] G. J. Borse, Numerical method with MATLAB, PWS Pub. Co., Boston, 1996.
[25] P. G. Lowe, Basic principles of plate theory, Chap. 3, Surrey Univ. Press, London 1982.
[26] A. N. Norris, "Flexural waves on narrow plates", Journal of Acoustic Society of America, vol. 113, issue 5, pp. 2647-2658, 2003.
[27] C. Vemula and A. N. Norris, "Flexural waves propagation and scattering on thin plates using Mindlin theory, Wave motion, vol. 26, issue 1, pp. 1-12, 1997.
[28] P. Šolín, Partial differential equations and the finite element method, section 6.5, Wiley & Sons, Hoboken, 2006.
[29] W. Flügge, Tensor analysis and continuum mechanics, Springer-Verlag, Berlin 1972.

Appendix A: Derivation of the identity relation (22)

Using the definition $\Delta_0 = \nabla \cdot \hat{1}\nabla$, one can derive,

$$\Delta_0 m_0 w = \nabla \cdot (w\hat{1}\nabla m_0 - \nabla w \cdot \hat{1} m_0) + m_0(\nabla \cdot \hat{1}\nabla w). \tag{A·1}$$

The same relation can be derived with use of $\hat{\upsilon}$ and $\hat{\tau}$ for $\hat{1}$ as follows,

$$\Delta_1 m_1 w = \nabla \cdot (w\hat{\upsilon}\nabla m_1 - \nabla w \cdot \hat{\upsilon} m_1) + m_1(\nabla \cdot \hat{\upsilon}\nabla w), \tag{A·2}$$

$$\Delta_2 m_2 w = \nabla \cdot (w\hat{\tau}\nabla m_2 - \nabla w \cdot \hat{\tau} m_2) + m_2(\nabla \cdot \hat{\tau}\nabla w). \tag{A·3}$$

In the similar procedur, the following identity can be derived

$$w\nabla \cdot (\rho I \nabla \ddot{u}) = \nabla \cdot (w\rho I \nabla \ddot{u}) - \nabla w \cdot \rho I \nabla \ddot{u}. \tag{A·4}$$

Summing up both hond sides of the relations from (A·1) to (A·4) and using the definitions (12) and (17), one can find

$$(\nabla \cdot \mathbf{s})w = m_0\Delta_0 w + m_1\Delta_1 w + m_2\Delta_2 w + \rho I \nabla \ddot{u} \cdot \nabla w + \nabla \cdot \left(\mathbf{s}w - M\nabla w\right). \tag{A·5}$$

In the steady state with an angular frequency ω, one can use the relation $\ddot{u} = -\omega^2 u$ in (A·5) and find the relation (22) to be bedemonstraited.

Appendix B: Derivation of coefficient matrices

The derivation of the coefficient matrices $\bar{c}_0$, $\bar{b}_0$, and $\bar{a}_0$ being introduced at (38) are summarized in this section. Using the Hermite interpolation functions L_r, N_r ($r = 0, 1$) and the variables $\eta_n = (y - nh_y)/h_y$ (n = -1,0) introduced in section 3.2, new two dimensional vectors $\mathbf{l}_n(y)$ (n=-1, 0, 1) are defined as follows,

$$\mathbf{l}_{-1}(y) = \begin{bmatrix} L_0(\eta_{-1}) \\ N_0(\eta_{-1}) \end{bmatrix}, \tag{A·6}$$

$$\mathbf{l}_0(y) = \begin{bmatrix} L_1(\eta_{-1}) + L_0(\eta_0) \\ N_1(\eta_{-1}) + N_0(\eta_0) \end{bmatrix}, \quad (A\cdot 7)$$

$$\mathbf{l}_1(y) = \begin{bmatrix} L_1(\eta_0) \\ N_1(\eta_0) \end{bmatrix}. \quad (A\cdot 8)$$

Then, the flexural deformation $u(x, y)$ and the arbitrary function $w(x, y)$ can be expressed as $u(x, y) = \sum_n \mathbf{l}_n(y) \cdot \mathbf{u}_n(x)$, $w(x, y) = \mathbf{l}_0(y) \cdot \mathbf{w}_0(x)$, where the definition of $\mathbf{u}_n(x)$ and $\mathbf{w}_0(x)$ are given in section 3.2. To obtain concise expressions, four-dimensional vectors $\mathbf{U}_n(x) = [\mathbf{u}_n(x)\ \frac{\partial}{\partial x}\mathbf{u}_n(x)]^T$ and $\mathbf{W}_0(x) = [\mathbf{w}_0(x)\ \frac{\partial}{\partial x}\mathbf{w}_0(x)]^T$ are introduced, then the integration with respect to y in the first term at the right hand side of (21) can be performed and a discretized expression is obtained as follows,

$$\begin{aligned}\int_{-h_y}^{h_y} dy m_0 \Delta_0 w &= \int_{-h_y}^{h_y} dy \Delta_0 w D_0 \Delta_0 u \\ &= \sum_{n=-1}^{1} \sum_{s=\pm 1} D_0^{(s)}(x) \Big[\mathbf{W}_0'(x)^T A_{00,ns} \mathbf{U}_n'(x) \\ &+ \mathbf{W}_0(x)'^T A_{20,ns} \mathbf{U}_n(x) + \mathbf{W}_0(x)^T A_{02,ns} \mathbf{U}_n'(x) \\ &+ \mathbf{W}_0(x)^T A_{22,ns} \mathbf{U}_n(x) \Big], \end{aligned} \quad (A\cdot 9)$$

where the dash, $'$, stands for the derivative with respect to x and $D_0^{(s)}(x) = D_0(x, sh_y/2)$. The following matrices are also used:

$$A_{00,ns} = \begin{bmatrix} O_2 & O_2 \\ O_2 & \langle \mathbf{l}_0 \mathbf{l}_n^T \rangle_s \end{bmatrix}, \quad (A\cdot 10)$$

$$A_{20,ns} = \begin{bmatrix} O_2 & \langle \mathbf{l}_0'' \mathbf{l}_n^T \rangle_s \\ O_2 & O_2 \end{bmatrix}, \quad (A\cdot 11)$$

$$A_{02,ns} = \begin{bmatrix} O_2 & O_2 \\ \langle \mathbf{l}_0 \mathbf{l}_n''^T \rangle_s & O_2 \end{bmatrix}, \quad (A\cdot 12)$$

$$A_{22,ns} = \begin{bmatrix} \langle \mathbf{l}_0'' \mathbf{l}_n''^T \rangle_s & O_2 \\ O_2 & O_2 \end{bmatrix}, \quad (A\cdot 13)$$

where O_2 is the 2×2 zero matrix, and the hat, $\langle \bullet \rangle_s$, is defined as follows,

$$\langle \bullet \rangle_s = \int_{-h_y}^{h_y} \bullet\, \theta(\eta_{(s-1)/2}) dy. \quad (A\cdot 14)$$

With a similar manner, using the variable $\xi_\ell = (x - x_\ell)/h_x$ and the matrices composed of the Hermite interpolation functions such as ,

$$\Lambda_r(\xi) = \begin{bmatrix} L_r(\xi) E_2 & N_r(\xi) E_2 \\ \frac{\partial}{\partial x} L_r(\xi) E_2 & \frac{\partial}{\partial x} N_r(\xi) E_2 \end{bmatrix} \quad (A\cdot 15)$$

(r=0, 1 and E_2 is the 2×2 unit matrix), the four-dimensional column vectors $\mathbf{U}_n(x)$ and $\mathbf{W}_0(x)$ can be discretized and interpolated with respect to x as follows,

$$\mathbf{U}_n(x) = \sum_{\ell=0}^{N_x-1} \Big[\Lambda_0(\xi_\ell) \mathbf{U}_n(x_\ell) + \Lambda_1(\xi_\ell) \mathbf{U}_n(x_{\ell+1}) \Big], \quad (A\cdot 16)$$

$$\mathbf{W}_0(x) = \sum_{\ell=0}^{N_x-1} \Big[\Lambda_0(\xi_\ell) \mathbf{W}_0(x_\ell) + \Lambda_1(\xi_\ell) \mathbf{W}_0(x_{\ell+1}) \Big]. \quad (A\cdot 17)$$

Using the above listed expressions and executing the integration of (A·9) with respect to x, the following expression is obtained as a discretized expression of the functional:

$$\begin{aligned}\iint_S m_0 \Delta_0 w dx dy &= \int_{-a/2}^{a/2} dx \int_{-h_y}^{h_y} dy \Delta_0 w D_0 \Delta_0 u \\ &= \sum_{\ell=0}^{N_x-1} \mathbf{\Psi}_\ell^T \sum_{n=-1}^{1} \sum_{s=\pm 1} D_0^{(s\ell)} \hat{A}_{s\ell}^{(\Delta_0)} \mathbf{\Phi}_{n\ell}. \end{aligned} \quad (A\cdot 18)$$

Here, $D_0^{(s\ell)} = D_0^{(s)}(x_\ell)$, $\mathbf{\Phi}_{n\ell} = [\mathbf{U}_n(x_\ell)\, \mathbf{U}_n(x_{\ell+1})]^T$, $\mathbf{\Psi}_\ell = [\mathbf{W}_0(x_\ell)\, \mathbf{W}_0(x_{\ell+1})]^T$, and

$$\hat{A}_{ns\ell}^{(\Delta_0)} = \hat{A}_{22,ns\ell}^{00} + \hat{A}_{02,ns\ell}^{10} + \hat{A}_{20,ns\ell}^{01} + \hat{A}_{00,ns\ell}^{11}. \quad (A\cdot 19)$$

The matrices $\hat{A}_{pq,ns\ell}^{ij}$ are defined as follows,

$$\hat{A}_{pq,ns\ell}^{ij} = \dot{\Big\langle} \begin{bmatrix} \Lambda_0^{(i)T} A_{pq,ns} \Lambda_0^{(j)} & \Lambda_0^{(i)T} A_{pq,ns} \Lambda_1^{(j)} \\ \Lambda_1^{(i)T} A_{pq,ns} \Lambda_0^{(j)} & \Lambda_1^{(i)T} A_{pq,ns} \Lambda_1^{(j)} \end{bmatrix} \dot{\Big\rangle}_\ell, \quad (A\cdot 20)$$

with

$$\Lambda_0^{(i)} = \frac{d^i}{dx^i} \Lambda_0(\xi_\ell), \quad (i = 0, 1) \quad (A\cdot 21)$$

$$\dot{\langle} \bullet \dot{\rangle}_\ell = \int_{x_\ell}^{x_{\ell+1}} \bullet\, dx. \quad (A\cdot 22)$$

Following a similar procedure, the integration in each term at the functional definition (21) can be discretized and the following expressions are derived for Δ_r (r = 1,2):

$$\begin{aligned}\iint_S m_r \Delta_r w dx dy &= \int_{-a/2}^{a/2} dx \int_{-h_y}^{h_y} dy \Delta_r w D_r \Delta_r u \\ &= \sum_{\ell=0}^{N_x-1} \mathbf{\Psi}_\ell^T \sum_{n=-1}^{1} \sum_{s=\pm 1} D_r^{(s\ell)} \hat{A}_{ns\ell}^{(\Delta_r)} \mathbf{\Phi}_{n\ell}, \end{aligned} \quad (A\cdot 23)$$

where

$$\begin{aligned} \hat{A}_{ns\ell}^{(\Delta_1)} &= \hat{A}_{22,ns\ell}^{00} - \hat{A}_{02,ns\ell}^{10} - \hat{A}_{20,ns\ell}^{01} + \hat{A}_{00,ns\ell}^{11}, \\ \hat{A}_{ns\ell}^{(\Delta_2)} &= \dot{\Big\langle} \begin{bmatrix} \Lambda_0^T A_{11,ns} \Lambda_0 & \Lambda_0^T A_{11,ns} \Lambda_1 \\ \Lambda_1^T A_{11,ns} \Lambda_0 & \Lambda_1^T A_{11,ns} \Lambda_1 \end{bmatrix} \dot{\Big\rangle}_\ell, \\ A_{11,ns} &= 4 \begin{bmatrix} O_2 & O_2 \\ O_2 & \langle \mathbf{l}_0' \mathbf{l}_n'^T \rangle_s \end{bmatrix}. \end{aligned} \quad (A\cdot 24)$$

For the terms proportional to ω^2, one can derive

$$\begin{aligned} &\int_{-a/2}^{a/2} dx \int_{-h_y}^{h_y} dy \omega^2 \rho \Big(I \nabla w \cdot \nabla u + b w u \Big) \\ &= \omega^2 \sum_{\ell=0}^{N_x-1} \mathbf{\Psi}_\ell^T \sum_{n=-1}^{1} \sum_{s=\pm 1} \rho^{(s\ell)} \Big(I^{(s\ell)} \hat{B}_{ns\ell}^{(\nabla)} + b^{(s\ell)} \hat{B}_{ns\ell}^{(\times)} \Big) \mathbf{\Phi}_{n\ell}, \end{aligned}$$

(A·25)

where

$$\hat{B}^{(\varsigma)}_{ns\ell} = \left\langle \begin{bmatrix} \Lambda_0^T B^{(\varsigma)}_{ns} \Lambda_0 & \Lambda_0^T B^{(\varsigma)}_{ns} \Lambda_1 \\ \Lambda_1^T B^{(\varsigma)}_{ns} \Lambda_0 & \Lambda_1^T B^{(\varsigma)}_{ns} \Lambda_1 \end{bmatrix} \right\rangle_\ell, \tag{A·26}$$

with $B^{(\varsigma)}_{ns}$ ($\varsigma = \nabla,\ \times$) that is defined as follows,

$$B^{(\nabla)}_{ns} = \begin{bmatrix} \langle \mathbf{l}_0 \mathbf{l}_n^T \rangle_s & O_2 \\ O_2 & \langle \mathbf{l}_0 \mathbf{l}_n^T \rangle_s \end{bmatrix}, \tag{A·27}$$

$$B^{(\times)}_{ns} = \begin{bmatrix} \langle \mathbf{l}_0 \mathbf{l}_n^T \rangle_s & O_2 \\ O_2 & O_2 \end{bmatrix}. \tag{A·28}$$

Here, the following notations are used: $\rho^{(s\ell)} = \rho(x_\ell + h_x/2, sh_y/2)$, $b^{(s\ell)} = b(x_\ell + h_x/2, sh_y/2)$ and $I^{(s\ell)} = I(x_\ell + h_x/2, sh_y/2)$. Then, the functional $F[w,u]$ defined by (21) is discretized as follows,

$$F[w,u] = \sum_{n=-1}^{1} \mathbf{\Psi}_\ell^T \sum_{s=\pm 1} \sum_{\ell} \Big\{ \sum_{r=0,1,2} D_r^{(s\ell)} \hat{A}^{(\Delta_r)}_{n\ell} - \omega^2 \rho^{(s\ell)} \Big(I^{(s\ell)} \hat{B}^{(\nabla)}_{n\ell} + b^{(s\ell)} \hat{B}^{(\times)}_{n\ell} \Big) \Big\} \mathbf{\Phi}_{n\ell}, \tag{A·29}$$

where the size of matrices with the super hat, ˆ, is 8×8.

The wave propagating along the y-aixis involves signal traveling of $\mathbf{\Phi}_{n\ell}$ with respect to n. When the gross vector $\mathbf{\Phi}_n$ of $8(N_x+1)$ dimension is defined as the serially aligned components of $\mathbf{U}_n(x_\ell)$ ($\ell = 0, 1, 2, ..., N_y$), then the vector $\mathbf{\Phi}_{n\ell}$ is equivalent to the partial series made by termes from $(1+4\ell)$-th to $(8+4\ell)$-th elements of $\mathbf{\Phi}_n$. Taking care about the fact that $\mathbf{U}_n(x_\ell)$ is common for vectors $\mathbf{\Phi}_{n\ell}$ and $\mathbf{\Phi}_{n\,\ell+1}$ and considering the mapping rule included in the definition (A·29), one can define new matrices $\bar{A}_n$ and $\bar{B}_n$ of $4(N_x+1) \times 4(N_x+1)$ dimension and writes the functional $F[w,u]$ as follows,

$$F[w,u] = \mathbf{\Psi}^T \sum_{n=-1}^{1} (\bar{A}_n - \omega^2 \bar{B}_n) \mathbf{\Phi}_n. \tag{A·30}$$

Since the weak form theory requires that the condition $F[w,u] = 0$ must be satisfied for the arbitrary $\mathbf{\Psi}$ or equivalently for any $w(x,y)$, the vectors $\mathbf{\Phi}_n$ or $u(x,y)$ must satisfy the relation $\sum_n (\bar{A}_n - \omega^2 \bar{B}_n)\mathbf{\Phi}_n = 0$. Ultimately, the coefficient matrices $\bar{c}_0$, $\bar{b}_0$, $\bar{a}_0$ for the case $n = 0$ in the difference equation (38) can be derived as follows,

$$\bar{c}_0 = \bar{A}_{-1} - \omega^2 \bar{B}_{-1}, \tag{A·31}$$

$$\bar{b}_0 = \bar{A}_0 - \omega^2 \bar{B}_0, \tag{A·32}$$

$$\bar{a}_0 = \bar{A}_1 - \omega^2 \bar{B}_1, \tag{A·33}$$

and $\bar{c}_0^{(1)} = \bar{A}_{-1}$, $\bar{b}_0^{(1)} = \bar{A}_0$, $\bar{a}_0^{(1)} = \bar{A}_1$, $\bar{c}_0^{(2)} = \bar{B}_{-1}$, $\bar{b}_0^{(2)} = \bar{B}_0$, $\bar{a}_0^{(2)} = \bar{B}_1$. The expressions for arbitrary n can be easily obtained by translating the coordinate y such as $y \to y - nh_y$.

Appendix C: Analyitcal mode function for homogeneous waveguides

The analytic expressions of the mode shape function are considered when an acoustic waveguide is composed of a homogeneous elastic plate, which is an extension of Krichhoff theory [26] with respect to the rotary inertia.

When the plate is homogeneous, the governing equation (20) reduces to

$$\Delta_0^2 u + 2k_{\mathrm{m}}^2 \Delta_0 u - k_{\mathrm{EB}}^4 u = 0. \tag{A·34}$$

Here, $k_{\mathrm{m}} = (\omega^2 \rho I/2D)^{1/2}$, $k_{\mathrm{EB}} = (\omega^2 \rho b/D)^{1/4}$, and the compatibility condition (8) was used. The symbols D, I, b, ρ are defined in section 2 and those values are independent of coordinates. When the plane wave is traveling along the y-axis with the wave number k_y, the displacement $u(x,y)$ caused by the flexural motion is expressed as follows,

$$u(x,y) = X(x) e^{ik_y y}. \tag{A·35}$$

The mode function $X(x)$ defines the wave shape that is whether symmetric, $X_{sy}(x)$, or anti-symmetric, $X_{as}(x)$, under the inversion of the x-axis. The analytic form of the function takes the form

$$X_{\mathrm{sy}}(x) = c_1 \cos(k_x x) + c_2 \cosh(\gamma x), \tag{A·36}$$

for the symmetric mode and

$$X_{\mathrm{as}}(x) = d_1 \sin(k_x x) + d_2 \sinh(\gamma x), \tag{A·37}$$

for the anti-symmetric mode.

Substituting these mode functions for the $u(x,y)$ in (A·34) yields the following relations,

$$k_x^2 = \sqrt{k_{\mathrm{EB}}^4 + k_{\mathrm{m}}^4} + k_{\mathrm{m}}^2 - k_y^2, \tag{A·38}$$

$$\gamma^2 = \sqrt{k_{\mathrm{EB}}^4 + k_{\mathrm{m}}^4} - k_{\mathrm{m}}^2 + k_y^2. \tag{A·39}$$

Using the boundary conditions that the plate fringe is free, which means that $m_{xx} = 0$ and $s_x + \partial m_2/\partial y = 0$ at $x = \pm a/2$, the condition on the wave number k_y is given as follows,

$$-(\nu k_y^2 + k_x^2)\cos(\frac{k_x a}{2})[(2-\nu)k_y^2 - 2k_m^2 - \gamma^2]\gamma \sinh(\frac{\gamma a}{2}) = (\nu k_y^2 - \gamma^2)\cosh(\frac{\gamma a}{2})[(2-\nu)k_y^2 - 2k_m^2 + k_x^2] \times k_x \sin(\frac{k_x a}{2}) \tag{A·40}$$

for the symmetric mode and

$$(\nu k_y^2 + k_x^2)\sin(\frac{k_x a}{2})[(2-\nu)k_y^2 - 2k_m^2 - \gamma^2]\gamma \cosh(\frac{\gamma a}{2}) = (\nu k_y^2 - \gamma^2)\sinh(\frac{\gamma a}{2})[(2-\nu)k_y^2 - 2k_m^2 + k_x^2] \times k_x \cos(\frac{k_x a}{2}) \tag{A·41}$$

for the anti-symmetric mode. The coefficients c_1 and c_2 for the symmetric mode satisfy the following relation,

$$\frac{c_1}{c_2} = -\frac{(\nu k_y^2 - \gamma^2)\cosh(\frac{\gamma a}{2})}{(\nu k_y^2 + k_x^2)\cos(\frac{k_x a}{2})}, \tag{A·42}$$

and the coefficients d_1 and d_2 for the anti-symmetric mode satisfy the relation,

$$\frac{d_1}{d_2} = -\frac{(\nu k_y^2 - \gamma^2)\sinh(\frac{\gamma a}{2})}{(\nu k_y^2 + k_x^2)\sin(\frac{k_x a}{2})}. \qquad (A\cdot 43)$$

The S_0 mode is the fundamental symmetric mode that can be described approximately by the Bernoulli-Euler theory of one dimensional beams. The curves with the labels S_1 and A_1 in the Fig. 4 and Fig. 5 correspond to the higher order symmetric mode and ant-symmetric mode that are subjected to the conditions (A·40) and (A·41), respectively.